Heliyon 10 (2024) e31518

Contents lists available at ScienceDirect

Heliyon

journal homepage: www.cell.com/heliyon

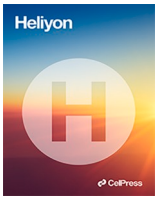

Research article

Extraction of flavonoids from black mulberry wine residues and their antioxidant and anticancer activity *in vitro*

Jian Ma [a,b,1], Peng Li [c,1], Yanhong Ma [a,b,e,**], Liya Liang [d], Feihong Jia [a,b], Yu Wang [b], Lijun Yu [a], Wuyang Huang [a,*]

[a] *Institute of Agro-Product Processing, Jiangsu Academy of Agricultural Sciences, No. 50 Zhongling Street, Nanjing, 210014, PR China*
[b] *College of Food Science and Engineering, Shanxi Agricultural University, Taigu, 030801, PR China*
[c] *Technical Center for Public Testing and Evaluation and Identification, Jiangsu Academy of Agricultural Sciences, Nanjing, 210014, PR China*
[d] *College of Agronomy & Resources and Environment, Tianjin Agricultural University, Tianjin, 300384, PR China*
[e] *The Work of Forestry Administrative Station of Kirgiz Autonomous Prefecture, Artush, 845350, PR China*

A R T I C L E I N F O

Keywords:
Black mulberry wine residues
Flavonoids
Ultrasound-assisted enzymatic extraction
Antioxidant capacity
Anticancer
Apoptosis

A B S T R A C T

Enhancing the valorization of fruit processing by-products is pivotal for advancing the industry. Black mulberry wine residues, a by-product, contains some bioactive compounds, yet its antioxidant and anticancer potentials remain unverified. In this study, ultrasound-assisted enzymatic extraction was optimized by response surface methodology to obtain the flavonoids extracts from black mulberry wine residues, whose antioxidant capacity and anti-cancer activity *in vitro* was investigated. The results showed that under the optimal extraction conditions (enzyme ratio at pectinase:cellulose = 2:1, mixed enzyme concentration 0.31 mg/mL, enzymatic hydrolysis temperature 55.35 °C, enzymatic hydrolysis time 79.03 min, and ultrasonic time 22.71 min), the extracts from black mulberry wine residues (BMWR-E) reached 5.672 mg/g. At a concentration of 1.2 mg/mL, BMWR-E exhibited strong DPPH and hydroxyl radical scavenging activities. At a concentration of 2.5 mg/mL, BMWR-E showed a strong superoxide anion radical scavenging capacity, with no significant distinction compared to the positive control group (Vitamin C) ($p > 0.05$). Cell viability assay results showed that BMWR-E was non-toxic to normal BRL-3A cells when applied at concentrations of 0.1–0.3 mg/mL for an incubation period of 24 h, but BMWR-E exhibited the ability to inhibit the proliferation of HepG2 cells. At concentrations of 0.2 mg/mL and above, BMWR-E could induce late apoptosis of HepG2 cells by increasing the protein expression levels of Bax, caspase-3, and caspase-12, reducing the protein expression levels of Bcl-2, inducing cell cycle arrest at G0/G1 phase, thereby inhibiting the proliferation of HepG2 cells. The bioactive properties make BMWR-E possess potential in developing new antioxidants and anti-cancer agents, which would significantly enhance the economic worth of agricultural by-products in product processing. This research can improve the utilization rate of agricultural product processing by-products and protect the environment.

* Corresponding author.
** Corresponding author. Institute of Agro-Product Processing, Jiangsu Academy of Agricultural Sciences, Nanjing, 210014, PR China.
E-mail addresses: mmmj001@163.com (J. Ma), li_sxnd@163.com (P. Li), ma_yhhyy@126.com (Y. Ma), liangliya@126.com (L. Liang), jfh19835147432@163.com (F. Jia), sxtgwy@126.com (Y. Wang), yulijun2002@163.com (L. Yu), wuyanghuang@hotmail.com (W. Huang).
[1] These authors contributed equally to this work.

https://doi.org/10.1016/j.heliyon.2024.e31518
Received 23 February 2024; Received in revised form 13 May 2024; Accepted 16 May 2024
Available online 18 May 2024

1. Introduction

Black mulberry (*Morus alba* L.), belonging to the Moraceae family, is an economic perennial herb grown in China, the United State, Brazil, and other places [1]. Compared with other colors of mulberries, black mulberries have higher content of bioactive substances, such as anthocyanins, polysaccharides, polyphenols, flavonoids [2,3]. Therefore, black mulberries have been confirmed to have antioxidant, anti-inflammatory, anti-tumor and other biological activities, and is a fruit with both edible and medicinal functions [4,5]. Black mulberries are usually processed into nutritious juice, pulp, wine, and other products, and its by-products account for 20 %–40 % of the fruit weight [6,7]. With the development of relevant processing technology, black mulberry products and hundreds of tons of by-products are processed on a large scale every year. These processing by-products are often discarded as animal feed or agricultural waste, causing a waste of resources and environmental pollution [8], which will become more and more serious.

Flavonoids, one category of phenolic compounds, are important secondary metabolites in plants with strong biological activity, which can reduce the risk of chronic diseases such as coronary heart disease, cancer, and type II diabetes [9–12]. The phenolic hydroxyl structure of polyphenols is easily oxidized into the quinone structure, which consumes oxygen and captures ROS, causing polyphenols to have a strong antioxidant function [13]. For example, quercetin's pentahydroxy structure gives it anti-inflammatory and anti-cancer properties, while the meta-5,7 dihydroxyl structure of green tea polyphenols and the di/trihydroxyl structure of B and D rings make it have various antioxidant activities [14,15]. The difference between isocatechin and epicatechin lies in the *cis*-trans conformation of site 2 and site 3, which results in a great difference in the biological activity function of the two [13]. Fruit processing by-products still contain a large number of flavonoids, which can be used as potential sources of functional nutraceuticals. Most studies on fruit processing by-products focus on kiwi fruits, grapes, raspberries, etc., but there are few related studies on black mulberry by-products [16–19]. In particular, the preparation process and biological activity of flavonoids in black mulberry wine residuals are still unclear.

Black mulberry wine residues (BMWR) is a by-product of black mulberry wine, which contains a lot of fiber and pectin, so the efficient extraction of flavonoids from BMWR requires technical assistance including biological enzymes. Enzymes with specific hydrolytic properties, e.g. pectinases and cellulases, are used to break down plant cell walls to obtain bioactive ingredients, such as flavonoids, within the cytosolic space. In order to ensure the complete break of the cell wall, various enzymes exhibiting complementary activities are more effective than a single enzyme [20,21]. Recent research has highlighted the efficacy of innovative technologies in facilitating the extraction of flavonoids and other bioactive compounds from natural sources [22]. These methods include enzyme-assisted extraction (EAE), ultrasound-assisted extraction (UAE), ultra-high-pressure-assisted extraction (UPE), and microwave-assisted extraction (MAE) [23–25]. Each technique offers a unique approach to enhance the efficiency and yield of extraction, harnessing the power of enzymes, ultrasound waves, extreme pressure, or microwave energy to unlock the bioactive substances of natural products [26]. The conventional methods have limitations, such as low yield, and are energy-intensive and associated with environmental problems [22]. These techniques are popular due to their high efficiency, short extraction duration, and easy operation process, especially ultrasound well known to enhance the rate of heat and mass transfer providing a high end-product quality, at just a fraction of time and energy normally required for conventional methods [27]. It has been reported that when UAE combined to EAE, the cavitation effect caused by the oscillation of stable cavitation bubbles may change the structure of surrounding enzymes, directly improve enzyme activity, enhance the contact between enzymes and substrates, and increase cell disruption and rapid mass transfer [28–31]. Therefore, ultrasound-assisted enzymatic extraction (UAEE) is also being developed as a new technique [32], which should be more efficient in extracting flavonoids from BMWR.

In the present study, UAEE technology was used to extract flavonoids from BMWR. Response surface methodology (RSM) was used to determine the optimum process conditions [33], and the antioxidant and anticancer biological activities of the extracts were evaluated. In addition, the effect of the extracts on the activity of normal cells and HepG2 cells was determined to determine the appropriate test concentration and incubation time. The effects of different concentrations of extracts on apoptosis rate and cell cycle of HepG2 cells were further determined, and the specific apoptosis pathways were verified by Western blotting. The outcomes of this study are expected to alleviate the environmental challenges posed by black mulberry wine residues while generating novel economic benefits.

2. Materials and methods

2.1. Materials

Black mulberry wine residuals (BMWRs) were provided by Wanshanhongbian Biotech Co., Ltd. (Jurong, Nanjing, China). After pre-frozen at −20 °C, the BMWR was dried in a freeze dryer (Laconic FreeZone-12, New York, USA) at −81 °C for 48 h. The freeze-dried samples were then ground using a JP-500C-6grinder (Long Products Industry & Trade Co., Ltd., Yongkang, China) and the dried powder was stored in an amber glass bottle at −20 °C.

2.2. Chemical and reagents

The reagents, including pectinase (EC 3.2.1.15), cellulase (EC 3.2.1.4), 1,1- dipheny1-2-picrylhydrazyl (DPPH), dimethyl sulfoxide (DMSO), and 3-(4,5-dimethylthiazol-2-yl)-2,5-diphenyltetrazolium bromide (MTT), were purchased from Sigma Chemical Company (St. Louis, MO, USA). Rutin standard (HPLC ≥98 %) and macroponous resin (HPD 300) (the purity ≥99 %) were purchased from Shanghai Source Leaf Biotechnology Co., Ltd. (Shanghai, China). Hydroxyl free radical kit and anti-superoxide anion free radical kit

were purchased from Jiancheng Biotechnology Co., Ltd. (Nanjing, China). Dulbecco's modified Eagle's medium (DMEM), PIMI-1640 medium, and fetal bovine serum (FBS) were purchased from GIBCO (Grand Island, NY, USA). Hoechst 33258 dye was purchased from Beyotime Institute of Biotechnology (Heimeng, China). Annexin V/PI apoptosis kit was purchased from MultiSciences Biotech Co., Ltd. (Hangzhou, China). All other chemicals and reagents used were analytical grade.

Rabbit monoclonal primary antibodies against β-actin, Bax, Bcl-2, caspase-3, caspase-12 were obtained from Santa Cruz Biotechnology Inc (Montana, USA). Secondary antibodies, goat anti-rabbit IgG-horseradish peroxidase (HRP, BA1054) conjugated antibody was bought from Boster Biotechnology Inc (Beijing, China). All primary antibodies were diluted 1000 folds and second antibodies 1500 fold except rabbit anti-Bax, which was diluted 1:600.

2.3. Extraction of flavonoids from BMWR by UAEE

According to a previous report, ultrasound-assisted enzymatic extraction of flavonoids was performed with some modifications [34]. The dried BMWR powder was degreased with petroleum ether and then dried. The defatted sample (0.5 g) was mixed with 5 mL of acidified distilled water (pH = 5.0). Then, pectinase plus cellulase were added to the mixture, respectively. After enzymolysis at 35–60 °C for 60–100 min, an additional 5 mL ethanol (final 50 % ethanol) was added to the mixtures at 300 W ultrasonic power using a KQ-2500E type ultrasonic instrument (Kunshan Ultrasonic Instruments Co., Ltd., Kunshan, China) for ultrasound-assisted extraction.

After extraction, the crude extract of flavonoids was filtered and separated, and concentrated in a RE-600 rotary evaporator (Shanghai Yarong Biochemistry Instrument Factory, Shanghai, China). The crude extract was purified using a activated HPD300 macroponous resin and desorbed using ethanol/water solution (70:30, v/v). The purified flavonoid extract was rotary evaporated to remove ethanol, freeze-dried for 24 h, and stored at −20 °C for analysis.

2.4. Determination of total flavonoids content

The total flavonoids content (TFC) was measured using the aluminum chloride colorimetric method as described by Yan et al. [35]. Absorbance was determined at 359 nm using a D-8 UV spectrophotometer (Shanghai Aoyan Scientific Instrument Co., Ltd., Shanghai, China). Rutin served as the reference standard, and the TFC was calculated based on the standard curve ($Y = 11.437\,X + 0.0096$, $R^2 = 0.998$). The TFC values were expressed as milligram of rutin equivalents per gram of BMWR (mg/g dry weight).

2.5. Single-factor experimental design

Using TFC as the evaluation index, the optimal technological conditions for extracting flavonoids from BMWR were selected. Among these conditions, the optimum enzyme combination was chosen from either pectinase (P), cellulase (C), or a blend of both enzymes in various mass ratios (PC, 1:1, 1:2, and 2:1). In the single-factor design, the following variable parameters were considered: the PC concentration (A: 0.1, 0.2, 0.3, 0.4, 0.5, and 0.6 mg/mL) with a mass ratio of 2:1 (w/w), enzymatic hydrolysis temperature (B: 35, 40, 45, 50, 55, and 60 °C), enzymatic hydrolysis time (C: 20, 40, 60, 80, 100, and 120 min), ultrasonic time (D: 5, 10, 15, 20, 25, and 30 min).

2.6. Box-Behnken design and analysis

Based on the outcomes of single-factor experiments, the following independent variables were selected for optimization through the Box-Behnken design (BBD) using response surface methodology (RSM): PC concentration (*A*: 0.2, 0.3, and 0.4 mg/mL), enzymatic hydrolysis temperature (*B*: 50, 55, and 60 °C), enzymatic hydrolysis time (*C*: 60, 80, and 100 min), and ultrasonic time (*D*: 15, 20, and 25 min). The TFC values (*Y*) were designated as the response variables for this optimization process. Design Expert version 8.0.6.1 (Stat-Ease Corp., Minneapolis, MN, USA) was employed to encode and integrate the different factor levels. The overall design encompassed a total of 29 experimental runs. The details of experimental variables, their coded levels, and the corresponding experimental results have been tabulated in Table S1.

2.7. Qualitative analysis of BMWR-E by liquid chromatography time of flight mass spectrometer (LC-TOF-MS)

In this study, a Shimadzu LC20 liquid chromatography system coupled with a Triple TOF™ 5600 + Q-TOF mass spectrometer (AB SCIEX, Foster, California, USA) was utilized for analysis. The BMWR-E sample was analyzed on a Waters XBridge C18 reversed-phase column (2.1 × 150 mm, 3.5 μm, Waters Corporation, Milford, Massachusetts, USA). The mobile phases consisted of solvent A (acetonitrile) and solvent B (0.1 % formic acid in water). The column was maintained at a temperature of 40 °C, with a flow rate of 0.3 mL/min and an injection volume of 3 μL. The gradient elution profile was as follows: 90 % B from 0 to 3 min; 90–0 % B from 3 to 25 min; 0 % B from 25 to 30 min; 0–90 % B from 30 to 30.1 min; 90 % B from 30.1 to 38 min. For detection, electrospray ionization (ESI) in both positive and negative ion modes was employed. The mass spectrometer parameters were set as follows: ion spray voltage was 5500 V for positive ion mode and −4500 V for negative ion mode; the ion source temperature was kept at 550 °C; the curtain gas was set to 35 psi; both gas 1 and gas 2 pressures were adjusted to 55 psi; the declustering potential was set at 80 V for positive ion mode and −80 V for negative ion mode; and the mass scan range was between 50 and 1200 Da. The MS/MS data acquisition was conducted in the Information Dependent Acquisition (IDA) mode with the following settings: collision energy (CE) was set to 40 eV for positive ion mode and −40 eV for negative ion mode, employing a rolling collision energy with a spread of 20 eV.

The mass spectrum data of BMWR-E were analyzed using Peakview 1.2 software (AB SCIEX, California, USA). To identify the components of BMWR-E, the experimentally obtained MS^2 data were cross-referenced against multiple databases, a local database as well as public resources like PubChem, Chemical Book (https://www.chemicalbook.com/), and the Mass Bank online databases. Through this comparative analysis, the compounds present in the BMWR-E sample could be tentatively identified and characterized.

2.8. In vitro antioxidant capacity

To assess the *in vitro* antioxidant capacity of BMWR-E, evaluations were carried out by determining their scavenging activities against DPPH (1,1-diphenyl-2-picrylhydrazyl) radicals, hydroxyl radicals, and superoxide anions. For these assays, the BMWR-E powder was dissolved and diluted to various concentrations (0.05, 0.20, 0.40, 0.60, 0.80, 1.00, and 1.20 mg/mL) with 70 % ethanol.

2.8.1. DPPH radical scavenging capacity assay

The DPPH radical scavenging capacity (DPPH-RSC) was evaluated following the previously reported method by Liu et al. [36]. Briefly, 0.1 mL aliquots of different concentrations were mixed with 0.05 mg/mL DPPH solution and allowed to react in the dark for 30 min. Subsequently, the absorbance at 517 nm was recorded using an iMake microplate reader (D-Epoch, Bio Tek Instruments, Inc, Vermont, USA). Vitamin C (Vc) was employed as a positive control for comparison. The DPPH scavenging percentage was computed according to the following formula:

$$\text{DPPH - RSC}(\%) = \left(1 - \frac{A_1 - A_2}{A_0}\right) * 100\%$$

where A_0 was the absorbance (Abs) of the mixed solution of absolute ethanol and the DPPH; A_1 was the Abs of the mixed solution of sample and the DPPH; A_2 was the Abs of the mixed solution of sample and absolute ethanol.

2.8.2. Hydroxyl radical scavenging capacity assay

The hydroxyl radical scavenging capacity (OH-RSC) was assessed by adhering to the guidelines provided in the hydroxyl radical determination kit. After performing the assay, the absorbance at 526 nm was read using the same iMake microplate reader (D-Epoch, Bio Tek Instruments, Inc., Vermont, USA). As with the DPPH-RSC assay, Vitamin C (Vc) was used as the positive control. The hydroxyl radical scavenging percentage was calculated with the following formula:

$$\text{OH} - \text{RSC}(\%) = \left(1 - \frac{A_1 - A_2}{A_0}\right) \times 100\%$$

where A_0 was the Abs of distilled water, A_1 was the sample's Abs, and A_2 was the Abs of distilled water instead of H_2O_2 solution.

2.8.3. Superoxide anion radical scavenging capacity assay

The superoxide anion radical scavenging capacity (SA-RSC) was quantified utilizing the protocol outlined in the anti-superoxide anion radical test kit. The absorbance at 550 nm was recorded using the iMake microplate reader (D-Epoch, Bio Tek Instruments, Inc., Vermont, USA). Distilled water acted as the blank control, while Vc served as the positive control. The superoxide anion radical scavenging percentage was calculated using the following formula:

$$\text{SA} - \text{RSC}(U/L) = \frac{A_1 - A_2}{A_1 - A_0} \times C_0 \times 1000$$

where A_1 was the Abs of the distilled water, A_2 is the sample's Abs, A_0 was the absorbance of the standard group, and C_0 was the standard concentration (U/L).

2.9. In vitro anti-cancer activity assay

2.9.1. HepG2 cell culture and treatment

The human hepatocellular carcinoma cell line, HepG2, and the normal hepatic liver cell, BRL-3A, were sourced from Shanghai Institute of Life Sciences, Chinese Academy of Sciences (Shanghai, China). The HepG2 cells were cultured in Dulbecco's Modified Eagle Medium (DMEM) supplemented with 10 % fetal bovine serum (FBS, v/v), 100 U/mL penicillin, and 100 μg/mL streptomycin under an atmosphere of 5 % CO_2 at a constant temperature of 37 °C. Meanwhile, the BRL-3A cells were grown in PRMI-1640 medium supplemented with the same proportion of FBS and antibiotics. Once both cell lines reached approximately 80 % confluence, they were treated with the flavonoids extract that had been appropriately diluted in the respective culture medium for further analysis.

2.9.2. Cell viability assay

The viability of HepG2 and BRL-3A cells was determined using the MTT assay [37]. In brief, cells were seeded into 96-well plates at a density of 2×10^4 cells per well. They were subsequently exposed to varying concentrations of the BMWR-E (0, 0.1, 0.2, 0.3, 0.4, and 0.5 mg/mL) for durations of 24, 48 and 72 h (h), respectively. Subsequently, 20 μL of MTT solution (5 mg/mL) was introduced to each well and allowed to incubate for 4 h. Upon removal of the supernatant from each well, the precipitate was dissolved in 150 μL of DMSO

and gently shaken for 10 min at 37 °C. The absorbance was then measured at 490 nm using the iMake microplate reader. The cell viability was calculated using the following formula:

$$\text{Cell viability}(\%) = \left(\frac{OD_{sample} - OD_{blank}}{OD_{control} - OD_{blank}}\right) * 100\%$$

where $OD_{control}$ is the cells without the flavonoids treatment, where OD_{blank} is only the medium, where OD_{sample} is the cells treated with the flavonoids.

2.9.3. Fluorescence microscopy (FM) observation

The HepG2 cells were treated with different concentrations of the BMWR-E (0, 0.1, 0.2, and 0.3 mg/mL) for a period of 24 h. Following this incubation, the cells were rinsed thoroughly with phosphate-buffered saline (PBS) and then subjected to staining with 10 μmol/L of Hoechst 33258 dye for duration of 15 min. This step allowed for the visualization of nuclear changes within the cells. Images of the stained HepG2 cells were subsequently captured using an IX53 Inverted Fluorescent Microscope (Olympus, Tokyo, Japan) equipped with 460 nm emission and 350 nm excitation filters, to discern structural alterations in the treated HepG2 cells.

2.9.4. Flow cytometric assay

The induction of apoptosis in HepG2 cells induced by BMWR-E was quantitatively determined using a BD FACS Calibur flow cytometer (BD Biosciences, San Jose, CA, USA). The cells were first incubated with different concentrations of the extracts (0, 0.1, 0.2, and 0.3 mg/mL) for a period of 24 h. Post-incubation, the HepG2 cells were harvested and stained with a freshly prepared mixture consisting of 20 μL AnnexinV-fluorescein isothiocyanate (FITC), 20 μL propidium iodide (PI), and 100 μL binding buffer. This mixture was then allowed to incubate at room temperature in the dark for 15 min. Following incubation, the samples were promptly analyzed on a Becton Dickinson (BD) FACS Calibur flow cytometer. AnnexinV-FITC was excited at 488 nm and PI at 546 nm. Cells exhibiting Annexin V fluorescence without or with PI staining were classified as early apoptotic or late apoptotic cells, respectively. Finally, the percentage of early apoptosis, late apoptosis, and the total apoptosis rate were calculated accordingly.

2.9.5. Cell cycle analysis

The HepG2 cells were plated in 6 well plates at a density of 5×10^5 per well and exposed to various concentrations of BMWR-E (0, 0.1, 0.2, and 0.3 mg/mL) for a 24-h incubation period. Following this, the cells were detached by trypsinization, washed with PBS, and then resuspended in 500 μL of PBS solution. Next, the cells were fixed in a 75 % ice-cold ethanol solution and stored at 4 °C overnight. Thereafter, the fixed cells were washed again with PBS and then treated with a mixture containing RNase A (100 μg/mL) and PI (50 μg/mL) in the dark for a 30-min incubation. Finally, the cell cycle progression was examined using the BD FACS Calibur flow cytometer, where PI-stained DNA content was detected and used to determine the distribution of cells across different stages of the cell cycle.

2.9.6. Western blotting

To assess the protein expression levels of Bax, Bcl-2, caspase-3, and caspase-12 in HepG2 cells, Western blotting analysis was conducted on cell lysates. β-Actin was utilized as an internal loading control to normalize the protein amounts across different samples. The protein bands were visualized using a LAS-3000 imaging system (Fuji, Tokyo, Japan). Subsequently, the band densities were quantified with the aid of Image J software (National Institutes of Health, Bethesda, Maryland, USA). Ultimately, all the obtained data were represented as fold changes relative to the control group.

2.10. Statistical analysis

All experiments were executed in triplicate to ensure reliability and precision, and the data obtained were expressed as the mean ± standard deviation (SD). Graphical representations of the data were generated using Origin 2020 software (Chicago, IL, USA). For the design and analysis of the response surface tests, Design-expert version 8.0.6.1 (Stat-Ease Corp., Minneapolis, MN, USA) was employed. Furthermore, statistical analyses, including the Analysis of variance (ANOVA), were carried out using IBM SPSS version 22.0 (Armonk, New York, NY, USA). In this study, statistical significance was determined when the p-value was less than 0.05.

3. Results and discussion

3.1. The screening of enzyme ratio

Previous studies have demonstrated that cellulases and pectinases can effectively disrupt cellular structure, thereby significantly enhancing the release of various bioactive compounds, including phenolic compounds, polysaccharides, oil, and others, from plant materials [21,38]. Here, the effects of cellulase (C) and pectinase (P), along with the different mass ratios of these two enzymes (PC, 1:1, 1:2, and 2:1), and their supplementary dosages on the flavonoid yield extracted from BMWR were investigated.

Fig. S1 illustrates that the flavonoid yield initially increased and then marginally decreased within a specific enzyme concentration range (0.1–0.6 mg/mL), with cellulase demonstrating a more pronounced effect compared to pectinase. Both the ratio and concentration of the enzymes significantly influenced the yield outcomes. It was observed that the complex enzyme system with a PC mass ratio of 2:1 proved to be the most efficacious in enhancing the extraction rate of flavonoids. This particular combination achieved the

highest TFC value of 5.22 mg/g among all the enzyme treatment groups ($p < 0.05$). Therefore, the PC ratio of 2:1 was selected as the appropriate enzymatic combination for further experiments.

3.2. Single-factor experimental analysis

Ultrasonic power and ultrasonic time significantly impact the extraction efficiency of bioactive substances, especially at 300 W, which is conducive to the release of flavonoids [39,40]. In addition, the appropriate temperature and duration can greatly enhance enzymatic hydrolysis efficiency [23]. Therefore, under the fixed condition of a 300 W ultrasonic power, the influences of PC concentration, enzymatic hydrolysis temperature, enzymatic hydrolysis time, and ultrasonic time on the flavonoid yield were analyzed.

Single-factor variations in PC concentration, enzymatic hydrolysis time, and ultrasonic time appeared to exhibit a positive correlation with the flavonoid yields, showing an increase as these variables rose and stabilizing at peak levels once optimal conditions were met (Fig. 1a-d). Under such conditions, a substantial amount of bioactive substances from plant cells would dissolve into the extraction solution, leading to a complete extraction of flavonoids [21,34]. However, regarding the factor of enzymatic hydrolysis temperature, the flavonoid yield initially increased but then started to decrease beyond a certain point. When the temperature exceeded 55 °C, enzyme activity was compromised, thus preventing the complete extraction of flavonoids [19].

According to the data presented in Fig. 1, the optimal parameters derived from single-factor tests included a mixed enzyme concentration of 0.3 mg/mL, an enzymatic hydrolysis temperature set at 55 °C, an enzymatic hydrolysis time of 80 min, and an ultrasonic time of 20 min. These identified optimal conditions could serve as a foundation for designing subsequent multivariate process optimization experiments.

3.3. Response surface optimization

3.3.1. Establishment of fitting model and analysis of variance

The quadratic response surface regression model was used to fit the data in Table S1, and the resulting quadratic multiple regression equation of flavonoid yield was obtained:

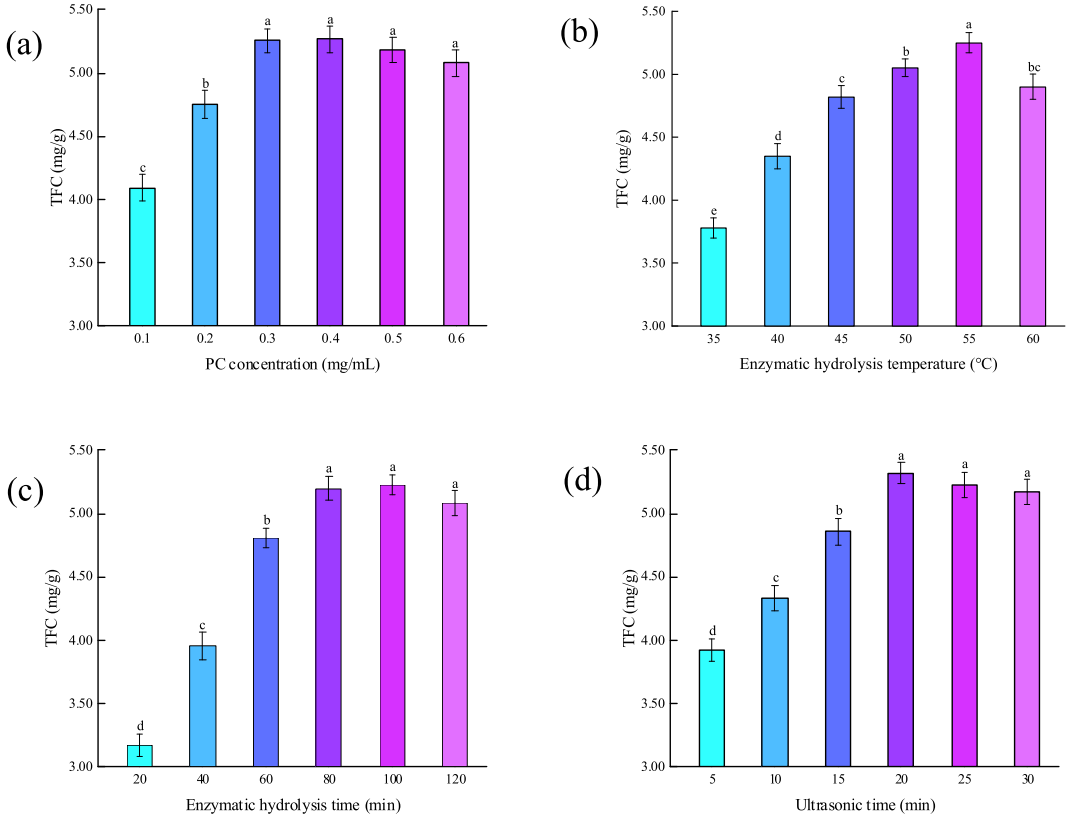

Fig. 1. Effects of different extraction parameters on the total flavonoid contents (TFC) of black mulberry wine residues (BMWR), (a) pectinase-cellulase (PC) concentration, (b) enzymolysis temperature, (c) enzymolysis time, (d) ultrasonic time. Bars represent mean values ± SD (n = 3). Different lowercase letters mean significant difference ($p < 0.05$).

$$Y = 5.48 + 0.14\,A + 0.083\,B + 0.018\,C + 0.67\,D + 0.22\,\mathrm{AB} - 0.25\,\mathrm{AC} - 0.19\,AD + 0.32\,\mathrm{BC} + 0.0025\,BD - 0.13\,CD - 0.42\,A^2 - 0.60\,B^2 - 0.52\,C^2 - 0.61\,D^2$$

Analysis of variance and significance test were used in regression model to validate its feasibility of the equation. The results are listed in Table 1. The *F*-value of model at 210.200 and *p*-value at 0.0001 conformed that each was coefficient, indicating the overall significance of the regression model [39]. The lack-of-fit with a *p*-value at 0.712 ($p > 0.05$) suggested that the loss was not statistically significant. The correlation coefficient R^2 (0.995) surpassed the threshold of 0.750 [38], suggesting that the data reasonably reflect the flavonoid yield. Furthermore, the predicted R^2 value (0.980), which closely aligned with the adjusted R^2 value (0.991), reinforced the precision and reliability of the developed model.

The ANOVA results from the model revealed that the mixed enzyme PC concentrations (*A*), enzymatic hydrolysis temperature (*B*), and ultrasonic time (*D*) exerted significant influences on the modelled flavonoid yield.

3.3.2. Response surface analysis

The flavonoids yields were analyzed when two variables were varied across their respective experimental range while the other factors were maintained at their optimal levels. The three-dimensional (3D) response surface plots representing the interactions of the four independent variables (extraction parameters) with the TFC are displayed in Fig. 2a-e.

Based on the principles of experimental design and the conducted data analysis, the 3D response surface graphs reveals that greater curvature typically signifies a more pronounced interaction effect between the two variables under consideration [40]. Fig. 2 effectively illustrates the impact of the interaction between every pair of parameters on the TFC. Fig. 2c and e show that ultrasonic time exerts the strongest influence on the TFC, while enzymatic hydrolysis time has the least discernible impact. Referring to Table 1, several pairs of variables exhibited display highly significant synergistic relationships, including the PC concentrations and enzymatic hydrolysis temperature (*AB*), the PC concentrations and enzymatic hydrolysis time (*AC*), the PC concentrations and ultrasonic time (*AD*), enzymatic hydrolysis temperature and enzymatic hydrolysis time (*BC*), enzymatic hydrolysis time and ultrasonic time (*CD*).

3.3.3. Verify the extraction process

As each factor increased, the flavonoid yield extracted from BMWR fluctuated accordingly, ultimately reaching a peak value on each response surface (Fig. 2). Based on these analyses, the optimal extraction process was established as follows: a PC concentration of 0.31 mg/mL, an enzymatic hydrolysis temperature of 55.35 °C, an enzymatic hydrolysis time of 79.03 min, and an ultrasonic time of 22.71 min. Three parallel experiments under these optimum conditions led to flavonoid extracts from BMWR achieving a yield of 5.672 mg/g, which did not differ significantly from the predicated yield. The results demonstrates that the utilization of response surface methodology to optimize the extraction process was indeed effective in extracting flavonoids from BMWR.

Table 1
Analysis of variance (ANOVA) for the experimental results.

Source	Sum of squares	Degree of freedom	Mean Square	*F* Value	*P*-value Prob > *F*	Inference
Model	11.632	14	0.831	210.200	<0.0001	**
A[a]	0.238	1	0.238	60.220	<0.0001	**
B	0.082	1	0.082	20.664	0.0005	**
C	3.680×10^{-3}	1	3.680×10^{-3}	0.930	0.3513	ns
D	5.320	1	5.320	1345.945	<0.0001	**
AB	0.193	1	0.194	48.980	<0.0001	**
AC	0.240	1	0.240	60.745	<0.0001	**
AD	0.148	1	0.148	37.500	<0.0001	**
BC	0.410	1	0.410	103.627	<0.0001	**
BD	2.500×10^{-5}	1	2.50×10^{-5}	6.325×10^{-3}	0.9377	ns
CD	0.070	1	0.070	17.767	0.0009	**
A^2	1.120	1	1.120	283.084	<0.0001	**
B^2	2.340	1	2.340	591.438	<0.0001	**
C^2	1.722	1	1.723	435.814	<0.0001	**
D^2	2.397	1	2.400	606.308	<0.0001	**
Residual	0.055	14	0.004			
Lack of fit	0.035	10	0.004	0.689	0.712	ns
Pure error	0.020	4	0.005			
Cor total[b]	11.687	28				
Std. Dev.[c]	0.063		R^2	0.995		
Mean	4.599		Adjusted R^2	0.991		
C.V.[d] %	1.367		Predicted R^2	0.980		
Press	0.233		Adeq Precision	44.726		

[a] A: PC concentration, mg/mL; B: enzymatic hydrolysis temperature, °C; C: enzymatic hydrolysis time, min; D: ultrasonic time, min.
[b] Cor Total: Totals of all information corrected for the mean.
[c] Std. Dev: Standard deviation.
[d] C.V: Coefficient of variation.

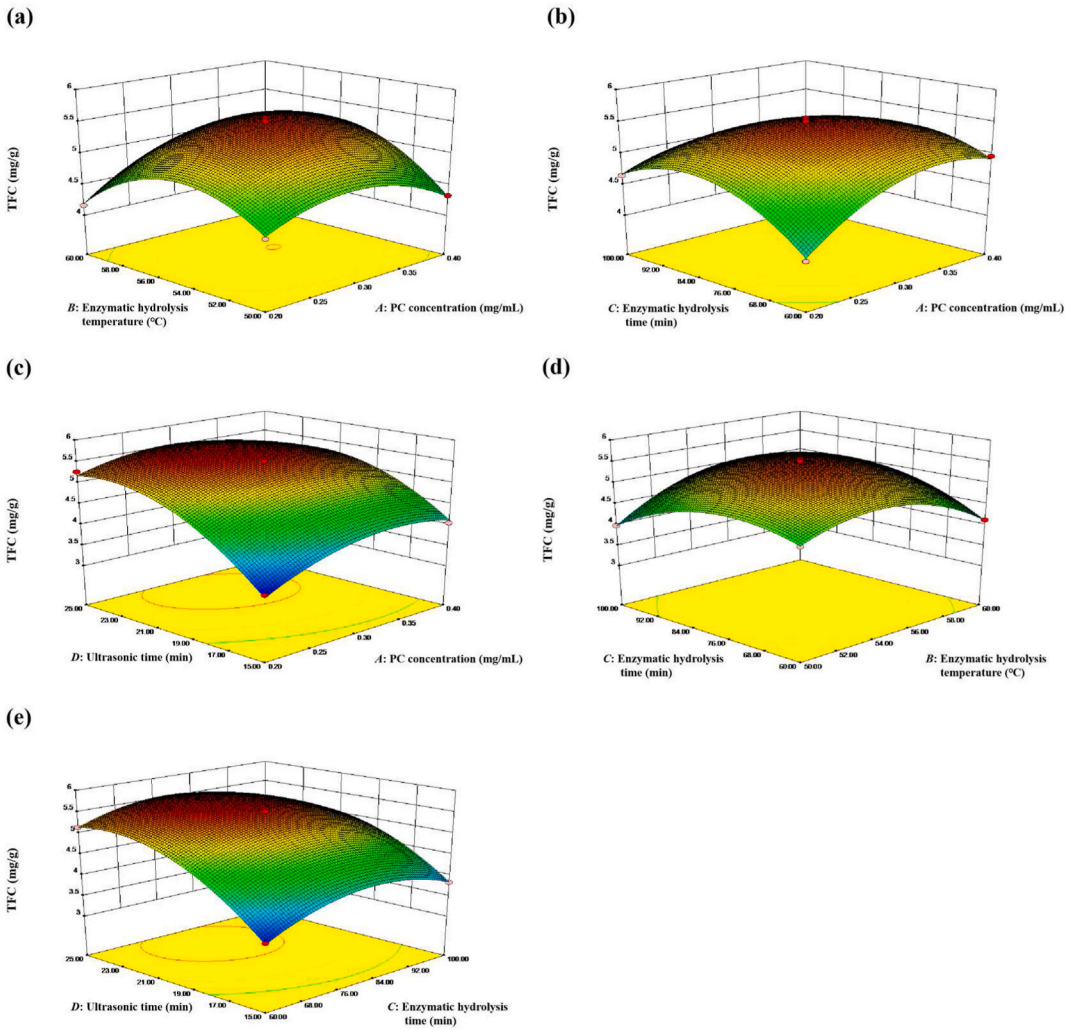

Fig. 2. Response surface analysis of the flavonoids extracted from BMWR (three dimensional response surface plots). (a) PC concentration and enzymatic hydrolysis temperature (*AB*); (b) PC concentration and enzymatic hydrolysis time (*AC*); (c) PC concentration and ultrasonic time (*AD*); (d) Enzymatic hydrolysis temperature and enzymatic hydrolysis time (*BC*); (e) Enzymatic hydrolysis time and ultrasonic time (*CD*).

3.4. Qualitative analysis of BMWR-E

As shown in Fig. S2, Fig. 3a-3l, and Table 2, a total of 12 distinct phenolic compounds (mainly flavonoids) were preliminarily identified in BMWR-E based on LC-TOF-MS analysis. The positive ion mode identified three major constituents, namely rutin, isoquercitrin, and petunidin 3-glucoside. On the other hand, the negative ion mode identified nine additional substances, including 3,4-dihydroxybenzaldehyde, cianidanol, taxifolin, hesperidin, neohesperidin, 6,7-dihydroxycoumarin, resveratrol, quercetin, and naringenin. The fundamental structure of flavonoids consists of a benzene ring (A ring) is linked through a pseudoring (C ring) to another aromatic ring (B ring), encompassing eight principal subclasses, flavones, flavonols, flavanones, flavanonols, flavanols (also known as catechins), anthocyanins, chalcones, isoflavonoids, and neoflavonoids [41]. Nine of the twelve compounds identified in the BMWR extract are flavonoids, including rutin, isoquercitrin, cianidanol, taxifolin, hesperidin, neohesperidin, quercetin, naringenin, and petunidin 3-glucoside. On the other hand, the remaining three compounds belong to different classes of phenolic compounds. 3, 4-Dihydroxybenzaldehyde is structurally categorized to phenolic acids, resveratrol is classified as a stilbene derivative, and 6,7-dihydroxycoumarin is a member of the coumarin family. Previous studies have shown that biological activity is largely determined by the number of groups that are easily oxidized, such as methoxy, hydroxyl, and carboxyl groups [13–15]. In Fig. 3, all the identified compounds possess a phenolic hydroxyl group, a characteristic feature that has been widely recognized for contributing to a myriad of bioactive properties, including cholesterol reduction, antioxidant capabilities, anti-cancer effects [9,10,29]. In the future, we will refine the extract's purity and employ molecular docking experiments to establish a clear structure-activity relationship, thereby substantiating the biological implications of these findings [15]. This approach will enable us to better understand how the chemical structure of these compounds influences their pharmacological actions and to potentially harness their therapeutic potential more

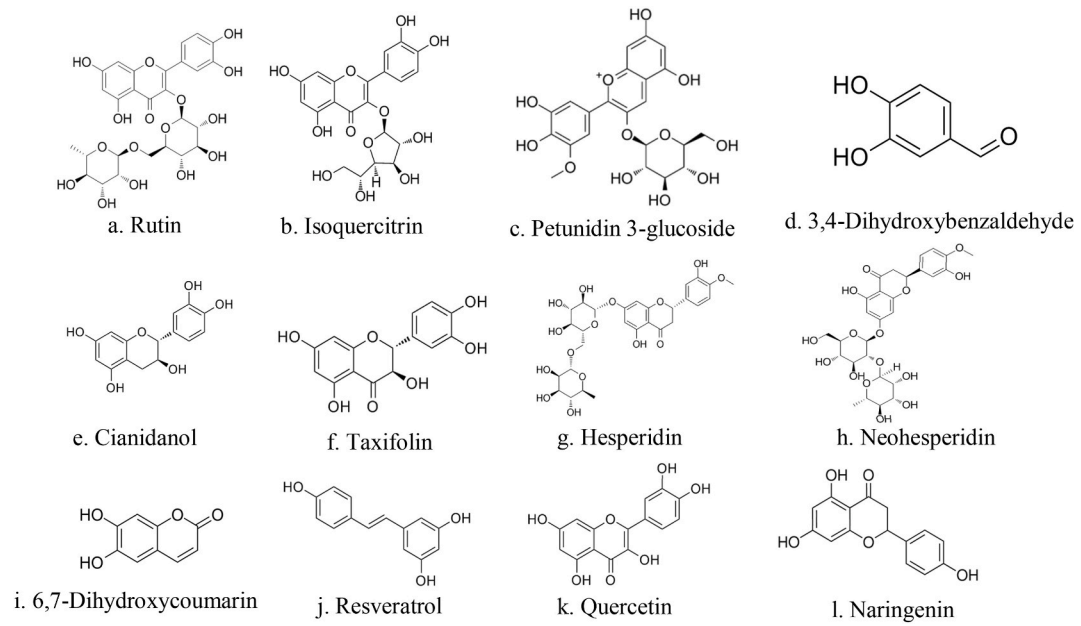

Fig. 3. The chemical structures of the twelve substances identified in BMWR-E. a. Rutin; b. Isoquercitrin; c. Petunidin 3-glucoside; d. 3,4-Dihydroxybenzaldehyde; e. Cianidanol; f. Taxifolin; g. Hesperidin; h. Neohesperidin; i. 6,7-Dihydroxycoumarin; j. Resveratrol; k. Quercetin; l. Naringenin.

Table 2
Qualitative results and analysis of the flavonoids extracted from BMWR.

Peak	Category	Identified substances	Rt (min) [a]	Precursor Ion (*m/z*)	[MS/MS] *m/z*
1	Flavonoids	Rutin	7.08	611.15 $^{+}$	303.05
2	Flavonoids	Isoquercitrin	7.33	465.10 $^{+}$	303.05
3	Flavonoids	Petunidin 3-glucoside	8.19	479.12 $^{+}$	317.07
4	Phenolic acid analog	3,4-Dihydroxybenzaldehyde	3.54	137.02 $^{-}$	108.03
5	Flavonoids	Cianidanol	3.71	289.07 $^{-}$	203.08
6	Flavonoids	Taxifolinl	6.78	303.05 $^{-}$	125.03
7	Flavonoids	Hesperidin	7.06	609.18 $^{-}$	300.05
8	Flavonoids	Neohesperidin	7.06	609.18 $^{-}$	300.05
9	Coumarin	6,7-Dihydroxycoumarin	7.46	177.02 $^{-}$	159.89
10	Stilbene	Resveratrol	9.18	227.07 $^{-}$	185.07
11	Flavonoids	Quercetin	9.91	301.04 $^{-}$	151.01
12	Flavonoids	Naringenin	10.73	271.06 $^{-}$	151.01

[a] RT: Retention time.

effectively.

3.5. Antioxidant activity of the BMWR-E

To comprehensively assess the antioxidant capacity of the BMWR-E extract, it is essential to employ multiple analytical techniques since no single method can provide a fully accurate representation. Among these methods, DPPH assay serves as an indicator of the antioxidant potential particularly associated with the B ring of flavonoids, which measures the ability of the flavonoids to stabilize DPPH free radicals by donating hydroxyl electrons from their hydroxyl groups [42]. The hydroxyl radical scavenging capacity assay focuses on the antioxidant properties that are mainly dependent on the structural features involving the B ring and a C2–C3 double bond conjugated with a C-3 hydroxyl group and a C-4 carbonyl group in flavonoids [42,43]. Additionally, the superoxide anion assay is mainly influenced by the structural elements like the 2, 3-double bond in the C-ring or the presence of ortho-dihydroxyl groups on B-ring of flavonoids. This is due to the fact that these specific functional groups allow the hydroxyl moiety to react with superoxide anions, forming stable complexes either via hydrogen bonding or covalent interactions. This mechanism effectively traps and neutralizes the superoxide anion, halting their participation in oxidative reactions and reducing oxidative stress [44]. Here, these three assays were applied to evaluate the antioxidant capacities of flavonoids extracted from BMWR.

In Fig. 4, the antioxidant capacity of the BMWR-E exhibits a dose-dependent increase. The DPPH-RSC values of BMWR-E was lower than those of the positive control Vc at the low concentrations ($p < 0.05$). However, upon reaching a concentration of 1.2 mg/mL, there was no significant difference between the DPPH-RSC values of rutin and Vc (Fig. 4a, $p > 0.05$). On the other hand, the OH-RSC values

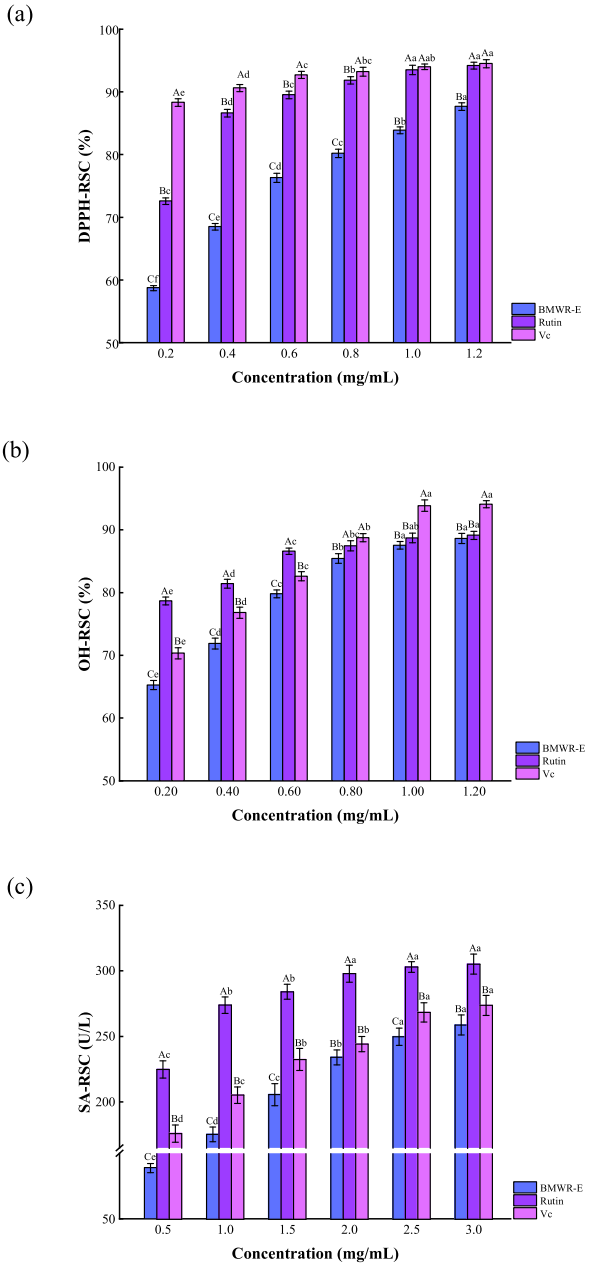

Fig. 4. Antioxidant capacity of the flavonoids extrated from BMWR-E, rutin and vitamin C (Vc) *in vitro*. (a) DPPH free radical scavenging ability (DPPH-RSC); (b) hydroxyl radical scavenging ability (OH-RSC); (c) superoxide anion scavenging abitily (SA-RSC). Bars represent mean values ± SD (n = 3). Different lowercase letters mean significant difference within groups ($p < 0.05$), while different capital letter means significant difference between groups ($p < 0.05$).

of rutin were notably higher than those of both BMWR-E and Vc at low concentrations ($p < 0.05$). However, when the concentration reached 1.2 mg/mL, there was no statistically significant distinction between the OH-RSC values of rutin and BMWR-E (Fig. 4b, $p > 0.05$), indicating that the extracts contains a substantial amount of rutin, which confers a potent hydroxyl radical scavenging capability. Intriguingly, when the concentration escalated above 2.5 mg/mL, the SA-RSC values of rutin were consistently higher than those of both BMWR-E and Vc ($p < 0.05$), and the SA-RSC values for all three groups all peaked, and at this point, the SA-RSC of BMWR-E became comparable to that of Vc (Fig. 4c, $p > 0.05$).

The results indicated that the flavonoids extract of BMWR had strong antioxidant capacity, which might be due to the hydroxyl structure of the compounds in its components. The accumulation of free radicals in organisms can cause oxidative stress reactions, leading to damage to DNA and proteins in cells, and inducing diseases such as cancer [9,36,37]. Antioxidants can prevent or slow down oxidative damage to cells by neutralizing free radicals, thereby exhibiting anti-cancer bioactive functions [17,42]. Subsequent cell

experiments were conducted to confirm the anti-cancer function of the extracts.

3.6. Effect of BMWR-E on cell viability

The liver cancer cell line HepG2 and normal hepatocytes BRL-3A were used to evaluate the antiproliferative effect of the BMWR-E using an MTT assay. The cells were both treated with various concentrations of BMWR-E (0.1, 0.2, and 0.3 mg/mL) for 24, 48, and 72 h, respectively.

In Fig. 5a, the BMWR-E effectively suppressed the viability of HepG2 cells in a dose- and time-dependent manner. Notably, concentrations exceeding 0.1 mg/mL of BMWR-E led to a significant decline in the proliferation rate of HepG2 cells, which was consistent with the findings reported by Lu et al. [45]. When HepG2 cells were treated with BMWR-E for 24 h, the cell viability rates decreased from 81.87 ± 3.25 % to 42.95 ± 3.33 % as the concentration of the extract increased. More substantial inhibitory effects were observed at concentrations above 0.2 mg/mL, and a longer stimulation period (72 h) resulted in significantly stronger suppression of cell viability compared to shorter periods (24 h) ($p < 0.05$). After 72 h of treatment with 0.50 mg/mL BMWR-E, the cell viability rate plummeted to merely 28.46 ± 2.22 %. The IC_{50} value of BMWR-E on HepG2 cells was 0.389, 0.235, and 0.204 mg/mL following 24, 48, and 72 h of incubation, respectively. This indicates that as the concentration of the BMWR-E extract rises, the viability rate of HepG2 cells correspondingly decreases, suggesting a potent antiproliferative effect of the extract against these liver cancer cells.

In contrast, the cell viability of BRL-3A cells showed no significant difference at low concentrations ranging from 0.1 to 0.2 mg/mL (Fig. 5b). Quercetin, a flavonoid compound, will produce cytotoxicity in normal cells when incubated with 0.25 mg/mL for 72 h [14]. But in this study, only higher concentrations and longer duration BMWR-E (≥0.3 mg/mL, 72 h) exhibited inhibitory effect on rat hepatocytes BRL-3A. The IC_{50} value of BMWR-E on BRL-3A cells were 0.823, 0.702, and 0.674 mg/mL for 24, 48, and 72 h of incubation, respectively. This was similar to the effects of curcumin on rat hepatocytes BRL-3A [46]. Moreover, it is known that the cytotoxic effects of phenolic compounds can be augmented through additive or synergistic effects [19,40,41], suggesting that the combined action of the phenolic compounds in BMWR-E might contribute to its potent inhibitory effect on HepG2 cell proliferation.

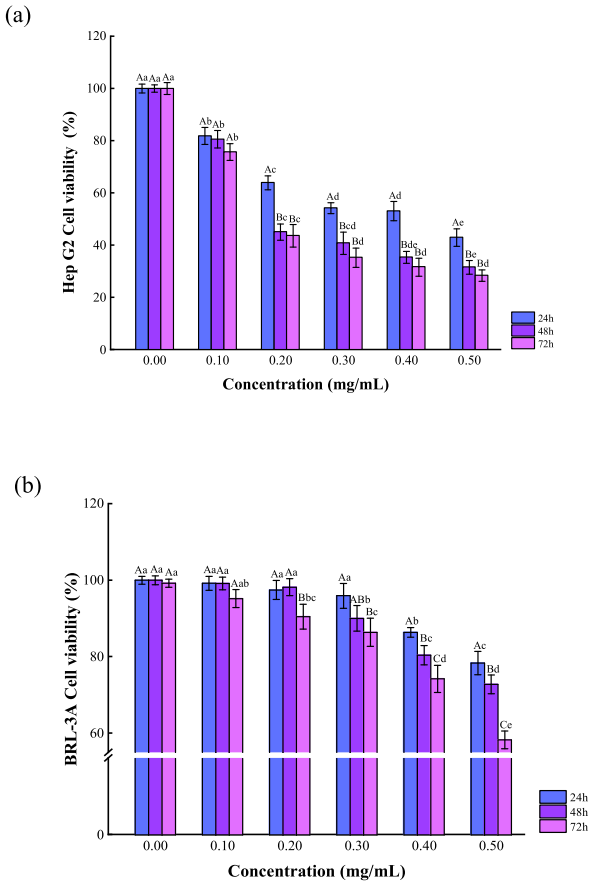

Fig. 5. Effect of the flavonoids extracted from BMWR on cell viability. (a) HepG2 cells; (b) BRL-3A cells. The cells were treated with various concentrations of BMWR-E (0, 0.1, 0.2, and 0.3 mg/mL) for 24, 48, and 72 h, respectively. Bars represent mean values ± SD (n = 3). Different lowercase letters mean significant difference within groups ($p < 0.05$), while different capital letter means significant difference between groups ($p < 0.05$).

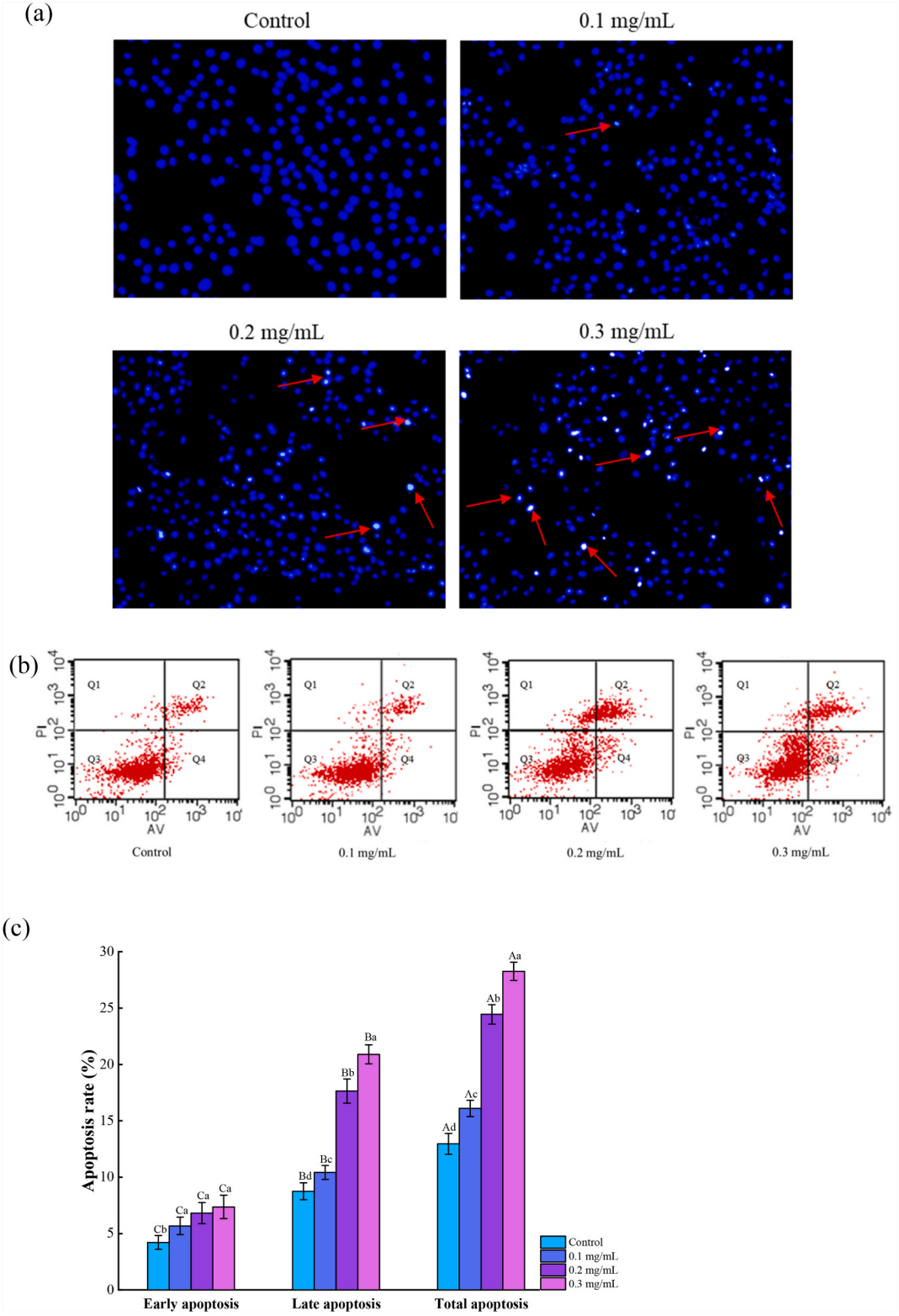

(caption on next page)

Fig. 6. Effect of the flavonoids extracted from BMWR on apoptosis rate of HepG2 cells. (a) Morphological changes; (b) flow cytometry analysis; (c) apoptosis rate. HepG2 cells were treated with various concentrations of BMWR-E (0, 0.1, 0.2, and 0.3 mg/mL) for 24 h. Hoechst 33258 staining in HepG2 cells was detected by fluorescence microscopy (FM). The nuclear DNA shows blue fluorescence. The red arrows indicate apoptosis cells showing nuclear condensation. All images presented are in × 200 magnification for FM. A representative set of images from three different independent experiments is shown. Apoptosis was measured by flow cytometry using annexin V and PI double staining. The Q1, Q3, Q2 and Q4 quadrant represent necrotic cells, viable cells, late apoptotic cells, and early apoptotic cells, respectively. Bars represent mean values ± SD (n = 3). Different lowercase letters mean significant difference within groups ($p < 0.05$), while different capital letter means significant difference between groups ($p < 0.05$). (For interpretation of the references to color in this figure legend, the reader is referred to the Web version of this article.)

The findings of this study indicated that BMWR-E selectively reduced the growth of HepG2 cells at varying concentrations without affecting the viability of normal liver cells like BRL-3A within a 48-h incubation period. Therefore, BMWR-E could be developed as a drug to inhibit HepG2 cell diseases. Consequently, these results support the potential development of BMWR-E as a candidate for drug therapy targeting HepG2 cell-related diseases, given its selective cytotoxicity and promising antiproliferative effects.

3.7. Effect of BMWR-E on apoptosis rate of HepG2 cells

In consideration of the high concentration of BMWR-E affecting normal liver cell viability, lower concentrations (0.1, 0.2, and 0.3 mg/mL) were selected to analyze its effect on HepG2 cell apoptosis.

HepG2 cell nuclei were stained with Hoechst 33258, and morphological changes in HepG2 cells treated with different concentrations of BMWR-E were observed by fluorescence microscope (Fig. 6a). Early morphological changes indicative of apoptosis, including chromatin condensation, cell shrinkage, and nuclear fragmentation, were observed in cells treated with the high concentration of BMWR-E (≥0.2 mg/mL) [45], and both cell volume and number decreased. The fluorescence intensity showed a progressive increase in the number of apoptotic bodies as the concentration of BMWR-E was augmented. The results suggested that the ability of BMWR-E to trigger apoptosis in HepG2 cells. The extent of cellular damage or apoptosis induction was directly proportional to the concentration of BMWR-E, which was further verified by flow cytometer analysis (Fig. 6b and c).

The early apoptotic rate increased from 4.21 ± 0.61 % to 7.36 ± 1.04 %, and there was a significant difference between the control and the samples ($p < 0.05$). The late apoptosis rate for the control was 8.75 ± 0.75 %. Upon treatment with increasing concentrations of BMWR-E, a significant change in the late apoptosis rate was observed ($p < 0.05$). The peak late apoptosis rate was achieved at a concentration of 0.3 mg/mL BMWR-E, escalating to 20.90 ± 0.84 %. The total apoptotic rates (combining early and late apoptosis)

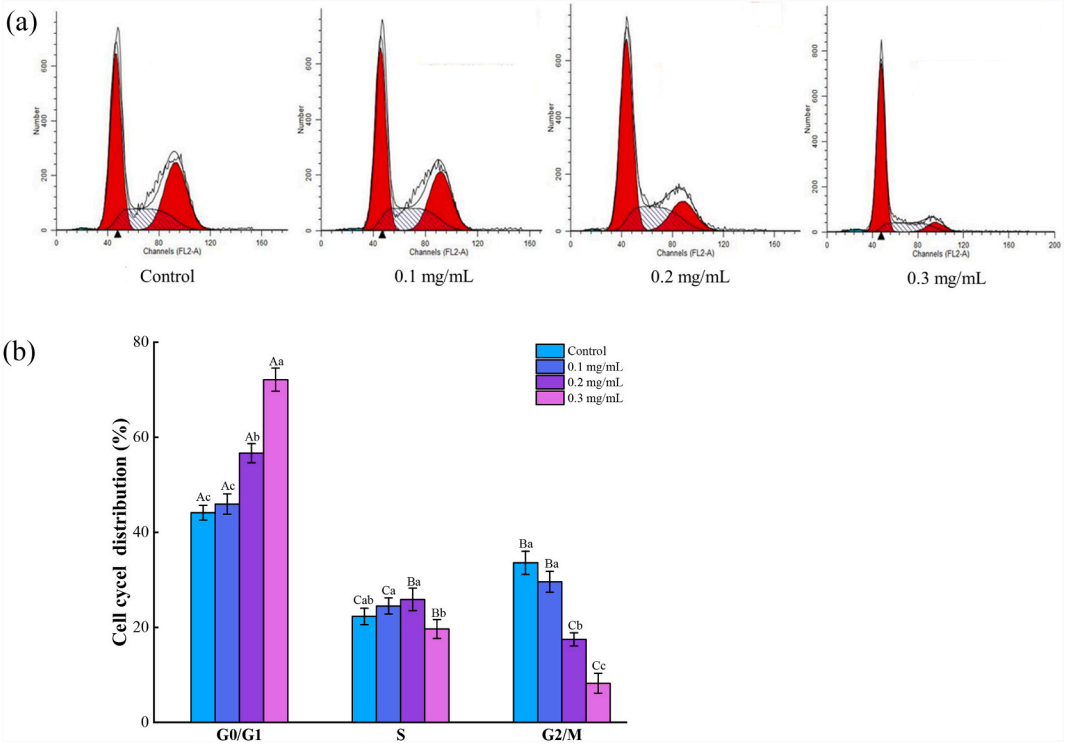

Fig. 7. Effect of the flavonoids extracted from BMWR on HepG2 cell cycle. (a) The changes of HepG2 cell cycle after treatment with different concentrations of the BMWR-E; (b) HepG2 cell cycle distribution. Bars represent mean values ± SD (n = 3). Different lowercase letters mean significant difference within groups ($p < 0.05$), while different capital letter means significant difference between groups ($p < 0.05$).

showed a marked increase in HepG2 cells as the concentration of BMWR-E rose, which jumped from 12.96 ± 0.92 % (the control) to 16.10 ± 0.72 %, 24.45 ± 0.86 %, and 28.26 ± 0.81 % for concentrations of 0.1, 0.2, and 0.3 mg/mL BMWR-E, respectively ($p < 0.05$, Fig. 6c).

In comparison to the BMWR-E, a separate study [45] investigated the effect of APSC polyphenols on HepG2 cells, treating them with a concentration of 0.4 mg/mL. The results from this study showed that the total apoptosis rate induced by APSC polyphenols was 23.11 ± 0.98 %. When juxtaposed with the current findings on BMWR-E, it appears that the latter demonstrates a higher efficacy in promoting apoptosis in HepG2 cells, as evidenced by the higher total apoptotic rates at equivalent or even lower concentrations. This suggests that BMWR-E might have a stronger pro-apoptotic effect on these liver cancer cells compared to the APSC polyphenols.

The results showed that the flavonoids extracted from BMWR caused HepG2 cell death mainly by inducing late apoptosis. Since early apoptosis is reversible and late apoptosis is irreversible, promoting the transition from early apoptosis to late apoptosis is beneficial for inducing apoptosis in tumor cells [37]. There are two pathways of apoptosis: the extrinsic death receptor pathway and the intrinsic mitochondrial pathway [46]. The detailed pathways inducing late apoptosis in HepG2 cell will be explored in subsequent studies.

3.8. Effect of BMWR-E on HepG2 cell cycle

Fig. 7a and b shows that the G0/G1 phase distribution of cells treated with BMWR-E increased from 44.13 ± 1.54 % to 72.13 ± 2.45 % with the sample concentration ranging from 0 to 0.3 mg/mL ($p < 0.05$). In addition, BMWR-E treatment at 0.2 mg/mL and 0.3 mg/mL significantly reduced the G2 phase percentage from 33.57 ± 2.44 % (in normal cells) to 17.47 ± 1.39 % and 8.21 ± 2.11 %, respectively ($p < 0.05$).

The high concentration of the BMWR-E (≥0.2 mg/mL) could induce cell cycle arrest at G0/G1 phase, thereby interfering with the cell cycle's progression into S phase. These results were similar to those reported by Cheol et al. [47] and Zhang et al. [48], but different from those of Zhou et al. [49], and Shan et al. [50]. G0/G1 cell cycle arrest can inhibit the proliferation of cancer cells and may be employed as a strategy in cancer treatment [47–50]. Treatment with bayberry leaf flavonoids has been shown to increase the expression of cleaved caspase-3 and -7, inducing apoptosis through ERK-dependent activation of caspase-9 within the intrinsic apoptosis pathway [48]. The results of flow cytometry analysis align with the findings of this study, suggesting that the apoptotic pathways involved may be similar.

3.9. Analysis of apoptosis-inducing pathway proteins

Caspase-12 is a key downstream executive protein in endoplasmic reticulum stress (ERS)-induced cell apoptosis [50]. Once activated, caspase-12 can stimulate the activation of cytoplasmic caspase-3, another crucial executioner protease in the apoptotic pathway. Caspase-3 has the ability to cleave sphingosine kinase 2 (SPHK2), which is released from cells and maintains its enzymatic activity outside the cell, regulating various cellular processes such as signal transduction and cell proliferation, and ultimately initiating cell apoptosis [48]. Additionally, Bcl-2 is an anti-apoptotic protein that acts to inhibit the initiation of apoptosis by preventing the release of cytochrome C (Cyt C) from the mitochondria into the cytosol. Cyt C is a cytochrome that participates in the electron transport chain and is an important part of the cellular respiration process. On the contrary, Bax is a pro-apoptotic protein that promotes mitochondrial outer membrane permeability, thereby facilitating the release of Cyt C [46]. The interplay between Bcl-2 and Bax is a key determinant of whether a cell survives or undergoes apoptosis, depending on the relative levels and activities of these two proteins. As shown in Fig. 8a-c and Fig. S3, with the increase in BMWR-E concentration, the protein expression of Bax, caspase-3, and caspase-12 protein increased, while the expression of Bcl-2 decreased. The Bax/Bcl-2 ratio is used to assess cell death or survival, reflecting the maintenance of mitochondrial membrane stability after apoptotic stimulation, and an increase in the ratio indicates an explosion of apoptosis [48]. In this study, the Bax/Bcl-2 ratios were 1.574 ± 0.051, 1.971 ± 0.031, and 3.506 ± 0.035 for BMWR-E concentration of 0.1, 0.2, and 0.3 mg/mL, respectively. This indicates that HepG2 cells had undergone apoptosis. Combined with Figs. 6 and 7, BMWR-E could induce late apoptosis in HepG2 cells by affecting the expression of apoptosis-related proteins. The primary constituents of jujube pulp polyphenols, ferulic acid and *p*-coumaric acid, can diminish the mitochondrial membrane potential (MMP) by inhibiting the AKT/NF-κB/Bcl-2 signaling pathway, thereby triggering the mitochondrial intrinsic apoptosis pathway and leading to apoptosis [50]. Similarly, BMWR-E comprises twelve phenolic compounds characterized by hydroxyl groups, benzene rings, and carboxyl structures [10]. These compounds have been shown to induce late-stage apoptosis in HepG2 cells, suppress the proliferation of cancer cells, and effectively contribute to cancer treatment strategies [9,15,50].

4. Conclusions

The extraction and utilization of bioactive substances from black mulberry wine residues represent an important way to resolve the waste of resources and environmental pollution. The results showed that under optimal extraction conditions, the extracts from black mulberry wine residues reached 5.672 mg/g. LC-TOF-MS identification revealed 12 kinds of phenolic compounds (primarily flavonoids) in the extracts, containing hydroxyl groups, carboxyl groups, benzene rings, and other easily oxidized groups, which contribute to their antioxidant capabilities. At a concentration of 1.2 mg/mL, the extracts exhibited strong DPPH and hydroxyl radical scavenging activities. At 2.5 mg/mL, they showed strong superoxide anion radical scavenging capacity. Furthermore, the extracts can induce cancer cell death by scavenging intracellular free radicals. At concentrations of 0.2 mg/mL and above, they could induce late apoptosis in HepG2 cells by increasing the protein expression levels of Bax, caspase-3, and caspase-12, and decreasing Bcl-2 expression, leading

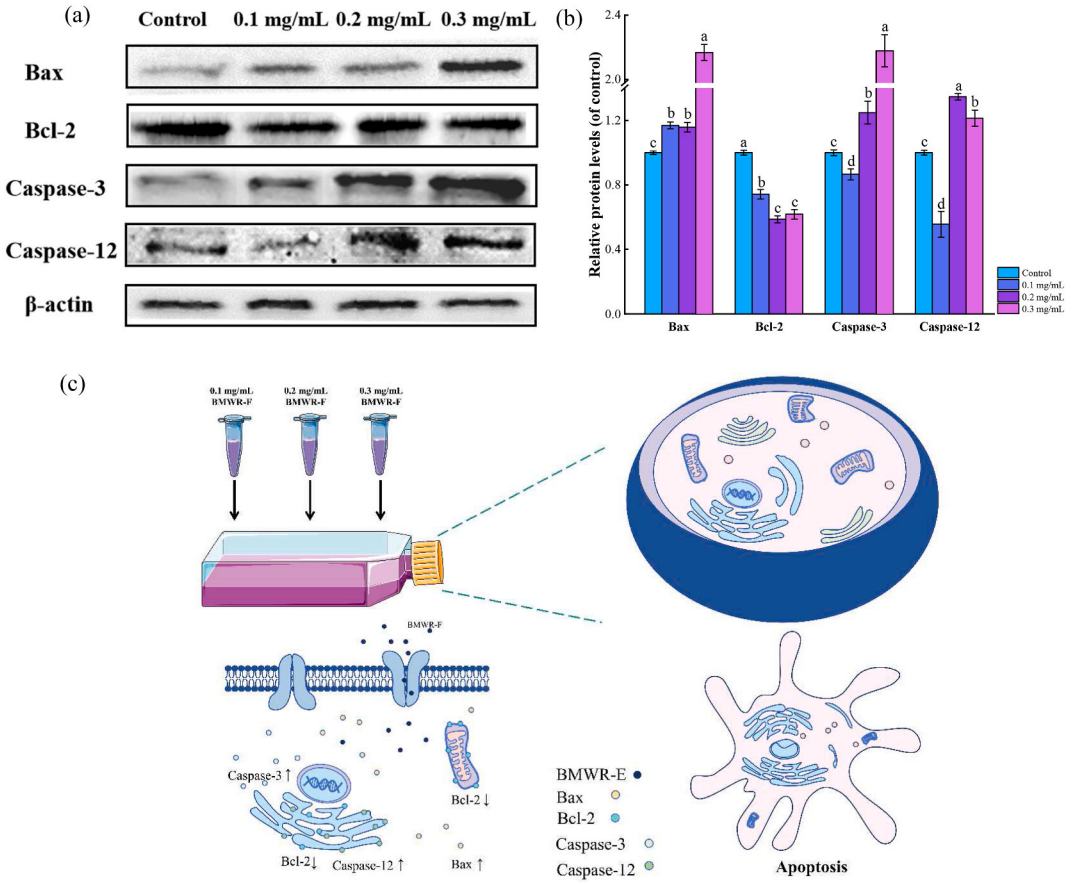

Fig. 8. Effects of the flavonoids extracted from BMWR on apoptotic protein content. (a) Electrophoretic diagram; (b) Bar diagram; (3) Mechanism diagram. HepG2 cells were treated with various concentrations of BMWR-E (0, 0.1, 0.2, and 0.3 mg/mL) for 24 h. Then, the effects of BMWR-E on the protein contents of Bax, Bcl-2, Caspase-3, and Caspase-12 were detected. Different lowercase letters mean significant difference within groups ($p < 0.05$).

to cell cycle arrest at the G0/G1 phase and thereby inhibiting the proliferation of HepG2 cancer cells. Therefore, black mulberry wine residuals would be used as antioxidant and anti-cancer functional food additive. Subsequent research will employ advanced separation techniques via preparative liquid chromatography for a precise evaluation of the anti-cancer properties of the extracts and their effects on various chronic diseases.

Ethical concern

There is no ethical part of the design of this experiment.

Availability of data and material

The datasets used and/or analyzed during the current study are available from the corresponding author on reasonable request.

CRediT authorship contribution statement

Jian Ma: Writing – original draft, Methodology, Investigation. **Peng Li:** Writing – original draft, Project administration, Conceptualization. **Yanhong Ma:** Validation, Resources, Funding acquisition, Data curation, Conceptualization. **Liya Liang:** Resources, Methodology. **Feihong Jia:** Validation, Supervision. **Yu Wang:** Data curation. **Lijun Yu:** Supervision, Investigation, Funding acquisition. **Wuyang Huang:** Writing – review & editing, Supervision, Project administration, Conceptualization.

Declaration of competing interest

The authors declare the following financial interests/personal relationships which may be considered as potential competing

interests:

Wuyang Huang reports a relationship with Heliyon that includes: board membership (An Associate Editor of the journal Heliyon—Food Science and Nutrition.

If there are other authors, they declare that they have no known competing financial interests or personal relationships that could have appeared to influence the work reported in this paper.

Acknowledgements

This research was supported by the Natural Science Foundation Project of Jiangsu Province [BK20191242] and the special project of Key research and development task of Xinjiang Autonomous Region [2023B02028-2]. We thank Dr. Chenye Yang from Central Laboratory in Jiangsu Academy of Agricultural Sciences for her technical support of LC-TOF-MS analysis.

Appendix A. Supplementary data

Supplementary data to this article can be found online at https://doi.org/10.1016/j.heliyon.2024.e31518.

References

[1] I. Khalifa, W. Zhu, K.K. Li, C.M. Li, Polyphenols of mulberry fruits as multifaceted compounds: compositions, metabolism, health benefits, and stability-A structural review, J. Funct.Foods 40 (2018) 28–43.
[2] C. Chen, L.J. You, A.M. Abbasi, X. Fu, R.H. Li, Optimization for ultrasound extraction of polysaccharides from mulberry fruits with antioxidant and hyperglycemic activity *in vitro*, Carbohydr. Polym. 130 (2015) 122–132.
[3] M.M. Natić, D.Č. Dabić, A. Papetti, M.M. Fotirić-Akšić, V. Ognjanov, M. Ljubojević, Ž.L. Tešić, Analysis and characterisation of phytochemicals in mulberry (*Morus alba* L.) fruits grown in Vojvodina, North Serbia, Food Chem. 171 (2015) 128–136.
[4] K. Li, H. Fan, P.P. Yin, L.G. Yang, Y.J. Liu, Structure-activity relationship of eight high content flavonoids analyzed with a preliminary assign-score method and their contribution to antioxidant ability of flavonoids-rich extract from *Scutellaria baicalensis* shoots, Arab. J. Chem. 11 (2) (2018) 159–170.
[5] E.M. Sánchez-Salcedo, P. Mena, C. Garcia-Viguera, J.J. Martinez, F. Hernandez, Phytochemical evaluation of white (*Morus alba* L.) and black (*Morus nigra* L.) mulberry fruits, a starting point for the assessment of their beneficial properties, J. Funct.Foods 12 (2015) 395–408.
[6] M. Tomas, G. Toydemir, D. Boyacioglu, R.D. Hall, J. Beekwilder, E. Capanoglu, Processing black mulberry into jam: effects on antioxidant potential and *in vitro* bioaccessibility, J. Sci. Food Agric. 97 (2017) 3106–3113.
[7] V. Samavati, M.S. Yarmand, Statistical modeling of process parameters for the recovery of polysaccharide from *Morus alba* leaf, Carbohydr. Polym. 98 (1) (2013) 793–806.
[8] A. Bhatnagar, M. Sillanpää, A. Witek-Krowiak, Agricultural waste peels as versatile biomass for water purification – a review, Chem. Eng. J. 270 (2015) 244–271.
[9] S.I. Ahmed, M.Q. Hayat, M. Tahir, Q. Mansoor, M. Ismail, K. Keck, R.B. Bates, Pharmacologically active flavonoids from the anticancer, antioxidant and antimicrobial extracts of Cassia angustifolia Vahl, BMC Compl. Alternative Med. 16 (1) (2016) 460.
[10] K.M. Brodowska, Natural flavonoids: classification, potential role, and application of flavonoid analogues, Eur J Bio Res 7 (2) (2017) 108–123.
[11] H.R. Sadeghnia, B.S. Yousefsani, M. Rashidfar, M.T. Boroushaki, E. Asadpour, G. Ahmad, Protective effect of rutin on hexachlorobutadiene-induced nephrotoxicity, Ren. Fail. 35 (8) (2013) 1151–1155.
[12] Y.P. Zhou, Dietary intake of flavonoid subclasses and risk of type 2 diabetes in prospective cohort studies: a dose–response meta-analysis, Clin. Nutr. 37 (6) (2018) 2294–2298.
[13] H.M. Yong, J. Liu, Polysaccharide-catechin conjugates: synthesis methods, structural characteristics, physicochemical properties, bioactivities and potential applications in food industry, Trends Food Sci. Technol. 145 (2024) 104353.
[14] S. Jing, X. Kong, L. Wang, H. Wang, J. Feng, L. Wei, Y. Meng, C. Liu, X. Chang, Y. Qu, J. Guan, H. Yang, C. Zhang, Y. Zhao, W. Song, Quercetin reduces the virulence of S. aureus by targeting ClpP to protect mice from MRSA-induced lethal pneumonia, Microbiol. Spectr. 10 (2) (2022) e0234021.
[15] Y. Zhou, S.G. Zheng, S. Yang, J.G. Li, K. Yang, J.F. Han, S. Duan, Green tea polyphenols alleviate β-conglycinin-induced anaphylaxis by modulating gut microbiota in rats, Food Biosci. 56 (2023) 103339.
[16] E. Agcam, A. Akyıldız, V.M. Balasubramaniam, Optimization of anthocyanins extraction from black carrot pomace with thermosonication, Food Chem. 237 (2017) 461–470.
[17] B. Fotschki, J. Juśkiewicz, A. Jurgoński, M. Kosmala, J. Milala, Z. Zduńczyk, J. Markowski, Grinding levels of raspberry pomace affect intestinal microbial activity, lipid and glucose metabolism in Wistar rats, Food Res. Int. 120 (2019) 399–406.
[18] K. Hamid, B. Saeid, Y.Q. Siew, Evaluation of bioactive compounds extracted from Hayward kiwifruit pomace by subcritical water Extraction, Food Bioprod. Process. 115 (2019) 143–153.
[19] M. María-Rocío, C. Ignacio, E.B. Carlos, R. Diana, Recovery of phenolic antioxidants from Syrah grape pomace through the optimization of an enzymatic extraction process, Food Chem. 283 (2019) 257–264.
[20] G. Octavia, M. Andrei, M. Cadmiel, L. Marcello, C. Gianina, C.F.R.F. Isabel, Enzyme-assisted extractions of polyphenols – a comprehensive review, Trends Food Sci. Technol. 88 (2019) 302–315.
[21] Z.H. Zhou, H.J. Shao, X. Han, K.J. Wang, C.P. Gong, X.B. Yang, The extraction efficiency enhancement of polyphenols from *Ulmus pumila* L. barks by trienzyme-assisted extraction, Ind. Crop. Prod. 97 (2017) 401–408.
[22] M. Gavahian, G.N. Mathad, R. Pandiselvam, J. Lin, D. Sun, Emerging technologies to obtain pectin from food processing by-products: a strategy for enhancing resource efficiency, Trends Food Sci. Technol. 115 (2021) 42–54.
[23] A. Boulila, I. Hassen, L. Haouari, F. Mejri, I. Ben-Amor, H. Casabianca, K. Hosni, Enzyme-assisted extraction of bioactive compounds from bay leaves (*Laurus nobilis* L.), Ind. Crop. Prod. 74 (2015) 485–493.
[24] S. Chen, H. Shang, J. Yang, L. Ran, H. Wu, Effects of different extraction techniques on physicochemical properties and activities of polysaccharides from comfrey (*Symphytum officinale* L.) root, Ind. Crop. Prod. 121 (2018) 18–25.
[25] V.M. Balasubramaniam, S.I. Martínez-Monteagudo, R. Gupta, Principles and application of high pressure–based technologies in the food industry, Annu. Rev. Food Sci. Technol. 6 (1) (2015) 435–462.
[26] A.A. Yüksel, A. Tuba, K. Alican, A. Furkan, K. Anjineyulu, R. António, A.A. Najla, R. Pandiselvam, Effect of ultrasound assisted cleaning on pesticide removal and quality characteristics of *Vitis vinifera* leaves, Ultrason. Sonochem. 92 (2022) 106279.
[27] A. Raouf, M.A. Shafiq, K. Jaspreet, P.A. Saeed, D.O. Iqbal, K. Anjineyulu, P. Ravi, Understanding the effects of ultrasound processing on texture and rheological properties of food, J. Texture Stud. 53 (6) (2021) 775–799.

[28] A. Görgüç, C. Bircan, F.M. Yılmaz, Sesame bran as an unexploited by-product: effect of enzyme and ultrasound assisted extraction on the recovery of protein and antioxidant compounds, Food Chem. 283 (2019) 637–645.
[29] F.J. Barba, Z.Z. Zhu, M. Koubaa, A.S. Sant'Ana, V. Orlien, Green alternative methods for the extraction of antioxidant bioactive compounds from winery wastes and by-products: a review, Trends Food Sci. Technol. 49 (2016) 96–109.
[30] P. Panja, Green extraction methods of food polyphenols from vegetable materials, Curr. Opin. Food Sci. 17 (2017) 173–182.
[31] J. Wang, Y.P. Cao, C.T. Wang, B.G. Sun, Low-frequency and low-intensity ultrasound accelerates alliinase-catalyzed synthesis of allicin in freshly crushed garlic, J. Sci. Food Agric. 91 (2011) 1766–1772.
[32] J. Wang, B. Sun, Y. Liu, H. Zhang, Optimisation of ultrasound-assisted enzymatic extraction of arabinoxylan from wheat bran, Food Chem. 150 (2014) 482–488.
[33] S. Çelik, N. Kutlu, Y.C. Gerçek, S. Bayram, R. Pandiselvam, N. Bayram, Optimization of ultrasonic extraction of nutraceutical and pharmaceutical compounds from bee pollen with deep eutectic solvents using response surface methodology, Foods 11 (22) (2022) 3652.
[34] L. Zhang, G.J. Fan, M. Ammar-Khan, Z. Yan, T. Beta, Ultrasonic-assisted enzymatic extraction and identification of anthocyanin components from mulberry wine residues, Food Chem. 323 (2020) 126714.
[35] L.G. Yan, Y. Deng, T. Ju, K.J. Wu, J. Xi, Continuous high voltage electrical discharge extraction of flavonoids from peanut shells based on "annular gap type" treatment chamber, Food Chem. 256 (2018) 350–357.
[36] S.J. Liu, C.E. Wu, G.J. Fan, T.T. Li, R.F. Ying, Y. Miao, Effects of yeast strain on anthocyanin, color, and antioxidant activity of mulberry wines, J. Food Biochem. 41 (6) (2017) e12409.
[37] Y.H. Ma, Y.H. Li, H.Z. Zhang, C.E. Wu, W.Y. Huang, Malvidin induces hepatic stellate cell apoptosis via the endoplasmic reticulum stress pathway and mitochondrial pathway, Food Sci. Nutr. 8 (9) (2020) 5095–5106.
[38] Z.Z. Liu, M.L. Gui, T.T. Xu, L. Zhang, L.T. Kong, L. Qin, Z.R. Zou, Efficient aqueous enzymatic-ultrasonication extraction of oil from *Sapindus mukorossi* seed kernels, Ind. Crop. Prod. 134 (2019) 124–133.
[39] M. Irakli, P. Chatzopoulou, L. Ekateriniadou, Optimization of ultrasound-assisted extraction of phenolic compounds: oleuropein, phenolic acids, phenolic alcohols and flavonoids from olive leaves and evaluation of its antioxidant activities, Ind. Crop. Prod. 124 (2018) 382–388.
[40] J.F. Song, Q.M. Yang, W.Y. Huang, Y.D. Xiao, D.J. Li, C.Q. Liu, Optimization of trans lutein from pumpkin (*Cucurbita moschata*) peel by ultrasound-assistedextraction, Food Bioprod. Process. 107 (2018) 104–112.
[41] W.Y. Huang, Y.Z. Cai, Y.B. Zhang, Natural phenolic compounds from medicinal herbs and dietary plants: potential use for cancer prevention, Nutr. Cancer 62 (2010) 1–20.
[42] P. Cos, L. Ying, M. Calomme, J.P. Hu, K. Cimanga, P.B. Van, L. Pieters, A.J. Vlietinck, D.V. Berghe, Structure−activity relationship and classification of flavonoids as inhibitors of xanthine oxidase and superoxide scavengers, J. Nat. Prod. (Lloydia) 61 (1) (1998) 71–76.
[43] G.R. Haenen, M.J. Arts, A. Bast, M.D. Coleman, Structure and activity in assessing antioxidant activity *in vitro* and *in vivo*: a critical appraisal illustrated with the flavonoids, Environ. Toxicol. Pharmacol. 21 (2) (2006) 191–198.
[44] J. Treml, Š. Karel, Flavonoids as potent scavengers of hydroxyl radicals, Compr Rev Food Sci F 15 (4) (2016) 720–738.
[45] C.R. Lu, C. Li, B. Chen, Y.H. Shen, Composition and antioxidant, antibacterial, and anti-HepG2 cell activities of polyphenols from seed coat of Amygdalus pedunculata Pall, Food Chem. 265 (2018) 111–119.
[46] G. Chen, Y.H. Wang, M.Q. Li, T.J. Xu, X.L. Wang, B. Hong, Y.C. Niu, Curcumol induces HSC-T6 cell death through suppression of Bcl-2: involvement of PI3K and NF-κB pathways, Eur. J. Pharmaceut. Sci. 65 (2014) 21–28.
[47] P. Cheol, J. Ji-Suk, J. Jin-Woo, O.K. Sung, H.C. Yung, Ethanol extract of *Kalopanax septemlobus* leaf inhibits HepG2 human hepatocellular carcinoma cell proliferation via inducing cell cycle arrest at G1 phase, Asian Pac. J. Tropical Med. 9 (4) (2016) 344–350.
[48] Y. Zhang, S.G. Chen, C.Y. Wei, G.O. Rankin, X.Q. Ye, Y.C. Chen, Flavonoids from Chinese bayberry leaves induced apoptosis and G1 cell cycle arrest via Erk pathway in ovarian cancer cells, Eur. J. Med. Chem. 147 (2018) 218–226.
[49] D.N. Zhou, A.H. Wei, C. Cao, J.L. Ruan, DICO, a novel nonaromatic B-ring flavonoid, induces G2/M cell cycle arrest and apoptosis in human hepatoma cells, Food Chem. Toxicol. 57 (2013) 322–329.
[50] S.H. Shan, Y. Xie, H.L. Zhao, J.P. Niu, S. Zhang, X.L. Zhang, Z.Y. Li, Bound polyphenol extracted from jujube pulp triggers mitochondria-mediated apoptosis and cell cycle arrest of HepG2 cell *in vitro* and *in vivo*, J. Funct.Foods 53 (2019) 187–196.